Vol. 21 — N°2 12 97 p. 279>287

GEOSTANDARDS NEWSLETTER
The Journal of Geostandards and Geoanalysis

Trace Element Determination of Single Fluid Inclusions in Quartz by Laser Ablation ICP-MS

Tom E. **McCandless** (1) David J. **Lajack** (2), Joaquin **Ruiz** (1) and A. Mohammad **Ghazi** (3)

(1) Centre for Mineral Resources, Department of Geosciences, University of Arizona, Tucson, Arizona 85721, USA
(2) Altar Resources, P.O. Box 1491, Nome, Alaska 99762, USA
(3) Department of Geology, Georgia State University, Atlanta, Georgia 30303, USA

Single fluid inclusions in quartz from a Pb-Zn-Ag carbonate replacement deposit were selected for trace element determination by laser ablation ICP-MS. Spikes in element intensities were noted between first breached fluids versus subsequent analyses, suggesting that accurate element concentrations may not be determined in smaller fluid inclusions when only one analysis is obtained before the fluid is exhausted. Elemental concentrations in the fluid inclusions were determined by external standardisation using solutions sealed in microcapillary tubes. Standards and single natural inclusion analyses give repeatabilities (%RSD) of ~ 20% for Rb and Sr. Rubidium and strontium concentrations range from 0.56-5.07 μg ml^{-1} and 1.12-27.4 μg ml^{-1}, respectively, whereas Zn and Ag are below detection limits (‹ 10 ng ml^{-1}). The results suggest that nearly all Zn and Ag are removed by the time hydrothermal fluids precipitate gangue minerals.

Des inclusions fluides provenant de quartz issus de minéralisations à Pb-Zn-Ag par remplacement de carbonates ont été selectionnées pour l'analyse in situ des éléments en trace par ICP-MS à ablation laser. Des sauts d'intensité ont été observés sur les signaux élémentaires lors de l'analyse de la première fraction de fluide extraite, par comparaison aux analyses suivantes. D'après cette observation, il ne serait pas possible d'obtenir des concentrations élémentaires justes sur les très petites inclusions, si une seule analyse peut être réalisée avant que l'inclusion ne soit vidée de son contenu. Les concentrations élémentaires dans les inclusions fluides ont été obtenues par calibration externe à l'aide de solutions scellées dans des tubes microcapillaires. Les analyses de standards et d'inclusions fluides individuelles naturelles donne des répétabilités (%ETR) de ~ 20% pour Rb et Sr. Les concentrations en rubidium et strontium varient dans une fourchette de 0.56-5.07 μg/ml et de 1.12-27.4 μg/ml, respectivement, alors que le Zn et l'Ag sont en dessous des limites de détection (‹ 10 ng/ml). Les résultats suggèrent que pratiquement tout le Zn et l'Ag ont déjà été extraits du fluide hydro-thermal lorsque les minéraux de la gangue précipitent.

Natural fluid inclusions have been analysed by a variety of non-destructive and destructive techniques (Roedder 1984). Non-destructive methods that have been used successfully for analysis of major elements in single inclusions include: synchrotron X-ray fluorescence (Frantz *et al.* 1988, Rankin *et al.* 1992, Vanko *et al.* 1993, Mavrogenes *et al.* 1995), proton induced X-ray emission (Horn and Tye 1989), and proton induced gamma-ray emission (Anderson *et al.* 1987). Destructive techniques can provide greater compositional information on the fluid inclusions and include laser microprobe noble gas mass spectrometry for analysis of halogens and the noble gases (Irwin and Roedder 1995), ion microprobe analysis of frozen inclusions (Kelly and Burgio 1983, Ayora and Fontarnau 1990, Nambu *et al.* 1977, Diamond *et al.* 1990), laser produced emission spectroscopy (Boiron *et al.* 1992) and laser ablation atomic emission spectroscopy (Rankin *et al.* 1992, Ramsey *et al.* 1992, Wilkinson *et al.* 1994). The low detection limit of ICP-MS and the ability of UV lasers to ablate IR-transparent host minerals such as quartz makes laser ablation ICP-MS (LA-ICP-MS) an ideal means of obtaining compositional information from single fluid inclusions (Ghazi *et al.* 1996, Moissette *et al.* 1996, Shepherd and Chenery 1995). We have developed a technique to quantify trace element concentrations in single fluid inclusions and have successfully analysed

Received 12 May 97 — Accepted 01 Jul 97

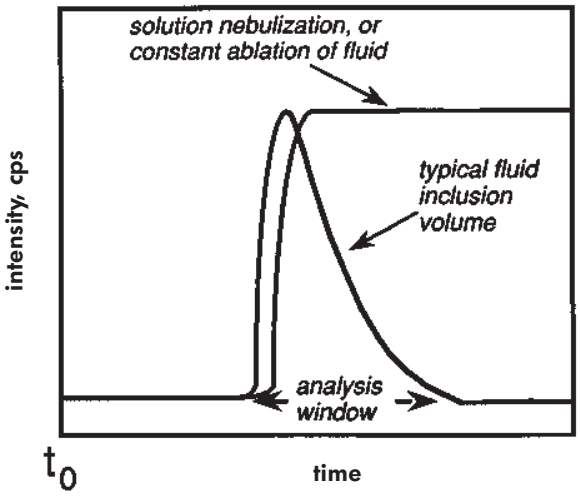

Figure 1. Schematic representation of signal intensity versus time for a solution measured by conventional nebulisation, compared to a natural fluid inclusion in a mineral. A solution measured by solution nebulisation can be considered 'infinite volumes' from which a large number of measurements can be obtained. Single fluid inclusions in minerals are extremely small volumes, limiting analysis time to a narrow window before the sample is completely consumed. The Santa Eulalia fluid inclusions are sufficiently large to allow for multiple analyses of the same inclusion (an opportunity to evaluate precision), or to ablate constantly to produce a steady signal like that shown for solution nebulisation.

single inclusions in halite from sedimentary basins in Texas and Colorado (Ghazi *et al.* 1996). In this study, we extend the technique to fluid inclusions from hydrothermal ore deposits.

Fluid inclusions in minerals from hydrothermal ore deposits are trapped at temperatures greater than 150 °C and at pressures of several hundred bars. Fluids trapped under these conditions develop a pressure differential relative to the ambient conditions found in a laser ablation cell. Thus, when the hydrothermal fluid inclusion is first breached by the laser, sudden pressure adjustments can affect signal intensity (e.g. spike or suppression relative to the true intensity) and lead to erroneous results (Shepherd and Chenery 1995). Unfortunately, most hydrothermal fluid inclusions are too small to allow multiple analysis of the fluid so that this possibility can be evaluated. Fluid inclusions in quartz from Santa Eulalia, Mexico are unique in that they are sufficiently large to allow a comparison between the first breached fluid, versus subsequent analyses from the same individual inclusion.

Another problem with the laser ablation ICP-MS analysis of single fluid inclusions is that repeatability is difficult to evaluate, again because the small volume of typical hydrothermal fluid inclusions seldom allows for replicate analysis. This problem is schematically expressed in Figure 1 where signal intensity for any element is plotted against time. In solution nebulisation ICP-MS, large volumes of sample provide a constant signal intensity, and enough measurements can be made to calculate statistically meaningful uncertainties. Single fluid inclusions are finite volumes, resulting in a narrow window of time for data to be collected before the sample is exhausted (Figure 1). Some Santa Eulalia fluid inclusions were so large that continuous ablation could be achieved for several minutes, with a steady signal to the detector (Figure 1). Integrated signal intensities measured under these conditions approximate results achievable by solution nebulisation ICP-MS, and allowed us to compare the integrated data with single analyses from the same fluid inclusion. The results provide some unique insights into the validity of single fluid inclusion data obtained by laser ablation ICP-MS.

Sample description

The Santa Eulalia Pb-Zn-Ag replacement deposit in northern Mexico hosts base metal sulfide mineralisation with associated silicate minerals precipitating from fluids at temperatures of 200-400 °C and pressures of 200-500 bars, respectively (Megaw 1990). The quartz crystals examined in this study formed late in the mineralisation sequence at Santa Eulalia. The euhedral crystals are 5-10 cm in length, with large vapour-liquid inclusions oriented parallel to the rhombohedral (1011) face, suggesting entrapment during primary crystallisation of the quartz (Figure 2A). Fluid volumes, estimated using a petrographic microscope, range from 0.10 to 52.0 μl, orders of magnitude larger than the 10^{-3} to 10^{-7} ml range for fluid inclusions typically observed in other hydrothermal ore deposits (Roedder 1984).

Instrumentation

Laser ablation system and ICP-MS

The laser ablation system used is the Finnigan-MAT System 266™ Nd:YAG laser, which operates at a wavelength of 1064 nm that is frequency quadrupled to 266 nm. The laser operates in Q-switched mode at pulse rates of 1-12 Hz, delivering a maximum energy of about 5 mJ per pulse at 266 nm. Real time ablation monitoring was achieved with the use of a

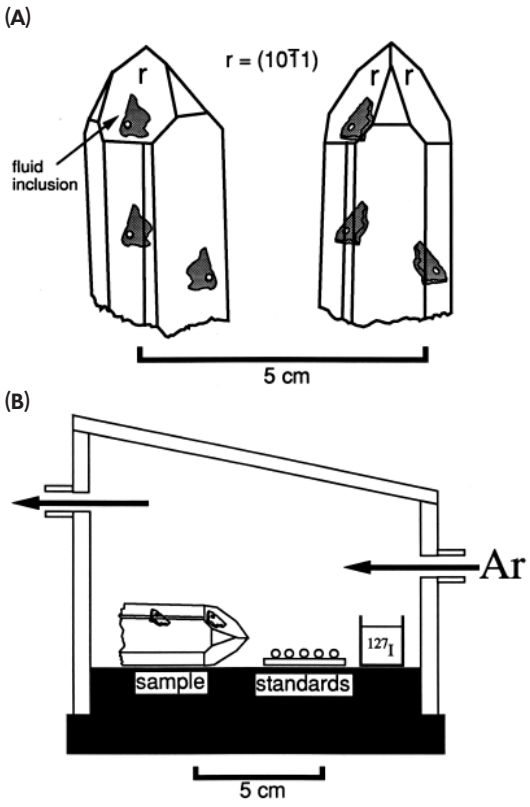

Figure 2. Representative quartz crystal with fluid inclusions from Santa Eulalia, Mexico. (A) Inclusions are oriented parallel to the (1011) face, suggesting primary origin. (B) Schematic arrangement of the laser ablation cell, showing the orientation of quartz sample, microcapillary tube standards, a 5 ml vial containing iodine tincture.

solid state CCD video camera and a colour monitor. The ablation chamber is a sealed 150 ml cylindrical housing composed of pyrex sides and a UV transparent quartz glass top (Figure 2B). Openings in the side of the sample ablation chamber were used for the introduction and exhaust of an argon carrier gas.

For this study, the Finnigan-MAT SOLA™ ICP-MS was used. In contrast to most laser ICP-MS configurations, the SOLA™ uses a dual gas flow system in which a solution is introduced into the ICP through peristaltic pumping and aspiration with argon through a concentric nebuliser. The ablated sample material is carried by an argon gas flow along a second line and mixes with aspirated water just prior to introduction into the plasma. This requires that the Ar pressure from the sample chamber is balanced with the nebuliser pressure to optimise signal intensity. To balance pressures such that the greatest possible amount of sample reaches the torch, a 5 ml vial of tincture of iodine (2% m/v I, 2.4% m/v NaI, 47% v/v isopropyl alcohol, 48.6% v/v H_20) is placed in the sample chamber (Figure 2B). The iodine tincture vapour is entrained in the Ar carrier gas, providing a steady ^{127}I signal which is monitored on the Faraday detector with the stage light off to avoid heating of the solution. Every time the chamber is opened and closed again, the ^{127}I mass is monitored on an analogue gauge to optimise the signal from the sample chamber to the torch.

Ions pass through sample and skimmer cones as in most ICP-MS, then through an accelerator cone, which produces a cross-over of the ion beam before introduction into the ion optics. The ions then pass through a conventional quadrupole mass filter to two detectors. A DC Faraday detector is used for ion beams greater than 10^6 ions s^{-1} (0.1-1 μg ml^{-1}), and the scanning electron multiplier (SEM) detector is the preferred detector for ion beams in the 1-10^6 ions s^{-1} range (~ 1-100 ng ml^{-1}).

Methods of analysis

The elements Zn, Ag, Rb and Sr were selected for this study. The quartz crystals were known to form late in the paragenetic sequence, and the measurement of Zn and Ag would indicate whether these base metals were removed from the fluids by this time. Rubidium and Sr were selected because they are relatively incompatible elements in igneous processes, and their presence in late fluid inclusions could suggest a similar behaviour under hydrothermal conditions. Masses ^{64}Zn, ^{85}Rb, ^{88}Sr, and ^{107}Ag were scanned during collection of data, which for the scanning conditions summarized in Table 1, required 25 seconds ablation time at 4 Hz.

Artificial fluid inclusion calibration samples

The use of micro-capillary tubes to hold standard solutions used in laser ablation ICP-MS analysis of fluid inclusions has been described in detail previously (Ghazi *et al.* 1996). Briefly, multi-element standard solutions were prepared by mixing of single-element SPEX standard solutions (SPEX Industries, USA). Artificial fluid inclusion standards were prepared by drawing 0.2-0.3 μl of a standard solution of known composition (50 and 25 μg ml^{-1} Cu, Zn, Sr and Rb in 2% v/v HNO_3) into 4 μl glass microcapillary tubes (Microcaps, Drummond Scientific, USA). The solution is drawn into the tube by capillary action such that void volumes are present on both ends of the tube, then the tube is carefully sealed with a jeweller's torch.

Table 1.
Typical operating conditions for the instrumentation used in this study

System 266 UV Laser	
Laser operating mode	Q-switched
Repetition rate	4 Hz
Output power	4 mJ/pulse
Ablation pit size	20 μm diameter
Focus condition	focus on surface
Stage argon flow rate	0.4 - 0.5 l min^{-1}
Total ablation time for analysis	25 s
SOLA ICP-MS	
Nebuliser flow rate	0.5 - 0.7 l min^{-1}
Extraction (potentiometer setting)	3.0
Pole bias (potentiometer setting)	7.0
Quadrupole resolution	37
Ion optics (potentiometer settings)	
X deflection	6.58
Y deflection	3.92
Y steer	6.85
Match	9.50
Focus	7.74
Acquisition mode	scanning
Mass resolution	16 channels amu^{-1}
SEM scanning conditions	1 scan, 8 passes
Acquisition time	15 s
Dwell time	16 ms

All data were collected in the Keck Trace Element Laboratory, University of Arizona.

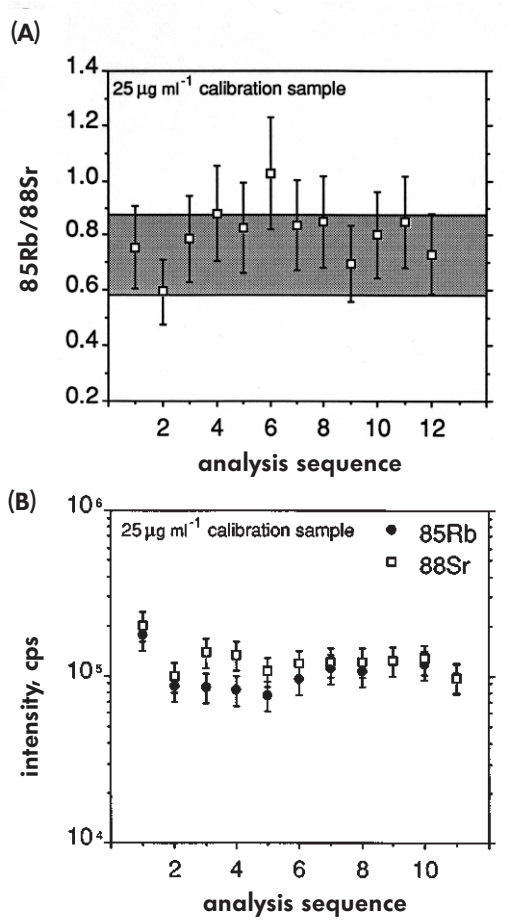

Figure 3. (A) $^{85}Rb/^{88}Sr$ ratios from a microcapillary tube calibration solution containing 25 μg ml l^{-1} each of Rb and Sr. (B) Intensities for ^{85}Rb and ^{88}Sr from a 25 μg ml l^{-1} microcapillary tube calibration solution.

Synthetic fluid inclusions in salts have been used as calibration samples in other studies of single fluid inclusions (Moissette *et al.* 1996). We prefer to use microcapillary tubes for the following reasons: (1) nearly all elements (except Si) are below detection in the glass; (2) the glass is inert to most solutions and will not allow elements in solution into its structure; (3) the exact concentration of the standard solution is known; (4) the solution is sealed into the tube at the same state conditions that it was made, i.e. no heating or precipitation is necessary to trap the fluid in its host; (5) the ablation characteristic of the glass is more similar to silicates than halite, the latter of which exhibits fracture along cleavage when first ablated (Ghazi *et al.* 1996); and (6) the volume of fluid consumed over a period of ablation can be calculated (Ghazi *et al.* 1996). This latter feature has an important bearing on the analysis of natural fluid inclusions, as discussed below.

At a selected distance from one meniscus of the liquid column, the laser is fired to ablate through the capillary tube wall, and ^{88}Sr is continuously monitored on the real time analogue gauge. Initial contact of the laser with the solution is marked by a jump in signal intensity, and individual measurements are taken. After each 25 second measurement, the laser beam is blocked with a mechanical gate switch until the ^{88}Sr signal returns to background (usually within a few seconds), then the procedure is repeated until the edge of the liquid meniscus advances to the hole created by the laser. A new ablation spot is selected at a distance from the previous hole, and a new set of measurements are obtained. Repeatabilities are +10-20% for Rb and Sr data obtained in this manner (Figure 3).

Since the inner diameter (Ø) of the microcapillary tube is accurately known to ~ 1%, and the number of laser pulses required to ablate a given length of fluid in the tube can be counted, the average volume of ablated fluid per pulse can be estimated:

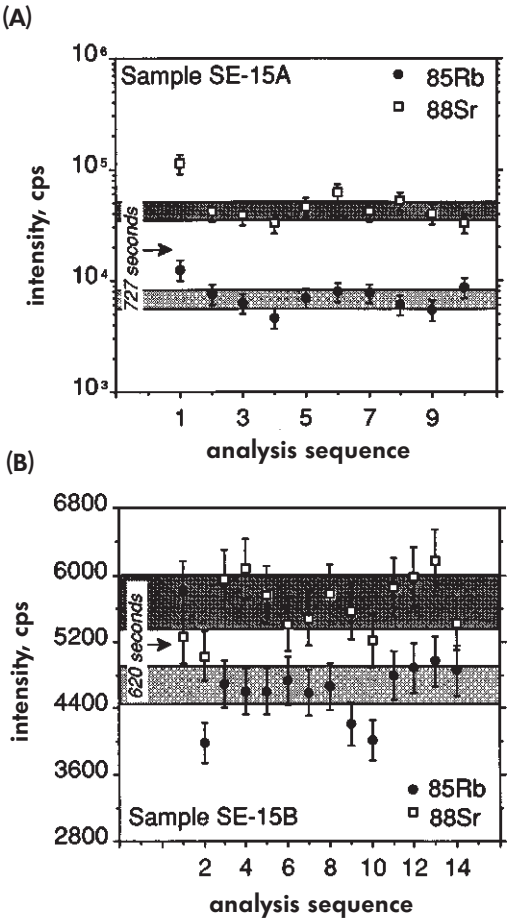

Figure 4. ^{85}Rb and ^{88}Sr signal intensities versus analysis sequence for two fluid inclusions in quartz SE15. Error bars are ±20%, time indicates total seconds elapsed for ablation of the quartz before the fluid inclusion was breached. Shaded areas indicate deviations about the mean for data collected during continuous ablation of the fluid inclusion, as explained in the text.

$$\frac{\text{(length of fluid)}\pi(1/2\varnothing)^2}{\text{(total pulses)}} = \text{volume of fluid/pulse.}$$

For the System 266, the volume is estimated at ~ 10^{-5} µl per pulse, for the operating conditions outlined in Table 1.

Natural fluid inclusions in quartz

No preparation of the quartz samples was necessary, other than cleaning the surfaces with ethanol, and marking the surface to be ablated with a permanent marker pen to aid in focussing the laser. The unknown, calibration samples and a 5 ml vial of tincture of iodine solution were placed in the chamber in the configuration shown in Figure 2B. The sample chamber argon flow to the ICP-MS was optimized using the ^{127}I solution as described previously. After analysis of the calibration sample, a fluid inclusion was located with the video monitor, and the laser was focused on the surface of the quartz. With the analogue gauge tuned to ^{88}Sr and multiplier detector selected, ablation was begun. When the ^{88}Sr signal jumped, scanning was immediately begun. The laser beam was blocked between each scan to allow the ^{88}Sr signal to return to background, then the procedure was repeated.

All data for each individual inclusion were collected from a single ablation hole in the quartz because in most cases, several minutes were required for the laser to ablate through the quartz and breach the inclusion wall (Figure 4). Between each 25 second analysis, the calibration sample solution was re-analysed to account for instrument drift, which for this study was negligible. With each new fluid inclusion, a new microcapillary tube standard was selected.

Concentrations of Rb, Sr, Zn and Ag were below detection limits in the quartz hosts, which was determined as ‹ 10 ng ml^{-1} based on a comparison of the ^{88}Sr signal intensity in the calibration sample to background intensities. The backgrounds were measured on quartz during ablation under the same conditions as for fluid inclusion analysis (Table 1).

Results

For the fluid inclusions in quartz, intensities were recalculated to concentrations in µg ml^{-1} by the following relation:

$$\frac{(Unk_{peak} - Unk_{background})}{(Cal_{peak} - Cal_{background})} \times (C_{cal}, \mu g\ ml^{-1}) = C_{unk}, \mu g\ ml^{-1}$$

where Unk is the intensity of the isotope mass measured in the unknown sample, Cal is the intensity of the same isotope mass measured in the microcapillary tube calibration sample, and C is the concentration of the element in the calibration sample solution. Concentration data for selected fluid inclusions are compiled in Table 2. Zinc and Ag are below detection in all inclusions.

Intensity data obtained for calibration samples and unknown samples are represented by individual points in Figures 3 and 4, respectively, with uncertainties of ± 20% assumed from the maximum uncertainties for the microcapillary tube standard measurements. Data were collected in the manner described above in order to imitate conditions when smaller fluid inclusions

Table 2.
Rubidium and strontium for two microcapillary calibration samples and for fluid inclusions in quartz

	Rb s^{-1}	Rb σ %	Sr s^{-1}	Sr σ %		
25 mg ml^{-1} standard-1	33717	10	36598	13		
25 mg ml^{-1} standard-2	136582	15	143983	11		
Sample (n)	**Rb μg ml^{-1}**	**Rb σ**	**Sr μg ml^{-1}**	**Sr σ**	**V μl**	**% vapour**
SE-4-1 (6)	1.80	0.31	0.52	0.09	11.0	9
SE-5A (6)	5.07	0.86	27.4	4.72	5.3	2
SE-5B (4)	0.56	0.10	1.12	0.19	1.0	11
SE-5C (5)	1.29	0.22	2.83	0.49	0.8	8
SE-15A (9)	3.40	0.59	2.45	0.42	14.0	6
SE-15B (10)	1.60	0.27	8.65	1.49	4.0	20

Calibration sample data are in counts per second for the element, with 1s uncertainties in percent. Sample concentrations are the average of (n) analyses, with 1s uncertainties in μl l^{-1} calculated at the maximum of 20%, based on repeatabilities of constantly ablated fluid inclusion standard solutions. Fluid inclusion volumes (in microlitres) and volume % of vapour are listed for each inclusion.

are analysed. Allowing the ^{88}Sr signal on the analogue gauge to return to zero meant that each analysis was limited to a finite volume of solution. However, an experiment was conducted in which the laser was fired continuously for several minutes into the calibration sample, and the ^{88}Sr signal was monitored. Under continuous firing, the ^{88}Sr would maintain relatively constant intensity in a manner similar to a nebulized solution, and similar behaviour was noted for the large volume fluid inclusions in quartz (Figure 1). Thus, it was possible to integrate a number of measurements from a signal intensity that approximated solution nebulisation ICP-MS, and compare the results to those obtained for finite volumes of the same fluid. The 1σ deviation about the mean of measurements obtained during continuous ablation is represented by the shaded areas in Figures 3 and 4.

Discussion

Manual vs time-resolved data collection

Many laser ablation ICP-MS systems have time-resolved software that permits continuous monitoring of a selected mass or masses during ablation. This option was not used, because the long ablation time before an inclusion is reached would make up the bulk of information collected in time-resolved mode. For example, 727 seconds were required to reach inclusion SE-15A, after which the first data are collected for approximately 25 seconds of ablation time (Figure 4A). Thus, we preferred the method of monitoring ^{88}Sr and starting the scan manually as outlined previously. One problem with the manual approach is that slow reflexes and/or a momentary inattention on the part of the operator may result in an inaccurate measurement.

One means of evaluating this uncertainty is to compare $^{85}Rb/^{88}Sr$ ratios for individual analyses to the deviation about the mean for the same solution analysed in continuous ablation mode (Figure 3B). The ideal $^{85}Rb/^{88}Sr$ ratio is 0.89 for equivalent ionisation of Rb and Sr and no mass fractionation. For the SOLA, the measured ratio during constant ablation of a 25 μg ml^{-1} microcapillary tube fluid is ~ 0.72 ± 20%, which may deviate from the ideal due to differences in ablation and ionisation efficiencies for Rb and Sr. The mean measured ratio and deviation are represented by the shaded region in Figure 3B. Individual points were obtained using the procedure as outlined in the text, with ± 20% error bars. Most of the points lie within the deviation about the mean for data obtained during continuous ablation (i.e. 11 of 12 points within shaded region). Assuming that the data collected during continuous ablation are the most representative, the manual procedure of data acquisition, represented by the individual points in Figure 3B, obtains results that are precise to ± 20% more than 90% of the time.

Variation in signal intensity

When a mineral host is ablated through, allowing the first ablation of a fluid inclusion, it is appropriate to ask

whether the first intensity measurement is enhanced or suppressed relative to subsequent intensity measurements for the element in question. This first measurement is referred to as the "first breach" intensity, i.e. when the walls of the inclusion are first breached and the fluid ablated. Hydrothermal fluids at temperatures near 400 °C and 200 bars may be expected to have densities as low as 0.5 g cm^{-3} near the critical end-point of H_2O (Norton 1984). When such a low density fluid is trapped in a hydrothermal mineral, the volume (and pressure) is held constant, but the density increases by as much as a factor of 2 when the mineral cools to ambient temperature. Thus, it is possible that the pressure is lower inside the fluid inclusion than in the sample chamber, which could cause a suppression of the vapour produced when the inclusion fluid is first ablated. Alternatively, fluids trapped in minerals near 200 °C and 200 bars experience only 10-20% increase in density at ambient temperatures, and the first breached fluid may be ablated without significant intensity fluctuation.

One way to evaluate the behaviour of first breach intensities in the absence of a pressure differential is to ablate a microcapillary tube calibration sample. In Figure 3A, each pair of points represents a measurement over approximately 25 seconds of ablation time of a 25 μg ml^{-1} standard solution. The uncertainties are ± 20%, which is the maximum deviation for a microcapillary calibration solution under constant ablation. Analysis number 1 in the sequence is the first breach analysis, which records a significant spike in signal intensity relative to subsequent measurements. This spike could be due to heating of the glass during prolonged ablation, such that the pressure increased slightly, resulting in a signal spike when the fluid is first breached. This example is exceptional in that the other microcapillary tube calibration samples used in this study had first breach intensities that were within the error of all subsequent measurements.

In comparison, the natural fluid inclusion sample SE-15A exhibits a significant spike for the first breach fluid, whereas subsequent analyses are within analytical uncertainty of the same fluid measured under continuous ablation (Figure 4A). Sample SE-15B also has a signal spike for the first breach fluid, with a cross-over of ^{85}Rb and ^{88}Sr intensities (Figure 4B). The results for SE-15A and 15B are not unique, and suggest that some aberration of signal intensity can occur for hydrothermal fluid inclusions analysed by laser ablation ICP-MS when they are first breached by the laser.

Density differences between calibration sample solution and natural fluid inclusions

One consideration in using external solutions for fluid inclusion calibrations is that different amounts of the unknown sample and calibration fluid are being ablated when compositional differences are sufficient to create density differences between the two fluids. The signal intensity I_a for a given element E in a weak acid can be expressed by the general relation:

$$I_a = k \bullet 4\ Hz \bullet V_a \bullet t \bullet C_{E,a} \bullet \rho_a$$

where t = time in s, 4 Hz is the laser pulse rate, k is the machine bias, V_a is the volume of acid ablated per pulse of laser, $C_{E,a}$ is the concentration of element E in the acid, and ρ_a is the density of the acid. The signal intensity I_b for the same element E in a brine can be expressed in a similar manner:

$$I_b = k \bullet 4\ Hz \bullet V_b \bullet t \bullet C_{E,b} \bullet \rho_b$$

where t = time in s, 4 Hz is the laser pulse rate, k is the machine bias, V_b is the volume of brine ablated per pulse of laser, $C_{E,b}$ is the concentration of element E in the brine, and ρ_b is the density of the brine. An ideal match between a calibration solution in a microcapillary tube and a natural fluid inclusion requires that $I_b = I_a$, or:

$$k \bullet 4\ Hz \bullet V_b \bullet t \bullet C_{E,b} \bullet \rho_b = k \bullet 4\ Hz \bullet V_a \bullet t \bullet C_{E,a} \bullet \rho_a.$$

All values are constant except volume and density, so if densities differ significantly, then a difference in the amount of material ablated must occur for the intensities to be equal. A 2% v/v HNO_3 solution has a density of about 1.01 g cm^{-3} whereas a brine with 15% m/v NaCl is 1.17 g cm^{-3}. This means that about 16% less volume is extracted in the brine versus the weak acid for each laser pulse. This correction factor of 16% is applied to the data in Table 2. For future studies in which one aim is to improve precision, microcapillary tube calibration solutions with NaCl accurately added to their composition will be used, a technique that is presently being investigated.

Application to smaller fluid inclusions

An interesting feature of using microcapillary tube calibration solutions is that the volume of ablated fluid per pulse of laser can be determined, which for the System 266 is 10^{-5} μl per pulse. To analyse four elements

using the parameters outlined in Table 1, 25 seconds of ablation time were required. The total volume consumed per individual analysis is then:

$$(25\ s) \bullet (4\ Hz) \bullet (10^{-5}\ \mu l/pulse) = 10^{-3}\ \mu l$$

These individual analyses represent volumes at the upper end of the range for natural hydrothermal fluid inclusions (10^{-3} to 10^{-7} µl; Roedder 1984). It is not possible to evaluate directly the repeatability for the analysis of the smallest measurable fluid inclusions, because insufficient material is available to undertake more than one analysis. However, repeatability can be estimated by comparing individual data points with the deviation about the mean for the same solution analysed under constant ablation conditions.

For natural fluid inclusions, each pair of points in Figure 4 was collected using the scanning procedure outlined above that would be necessary if single inclusions were being analysed. After all of the individual analyses were collected for each sample (points 1-10 Figure 4A, points 1-14 in Figure 4B), the laser was fired continually into each fluid inclusion and several analyses were collected and averaged. The dark stippled area represents the deviation about the mean for Rb, and the light stipple represents the deviation about the mean for Sr for data collected under continuous ablation mode. In Figure 4A, the first analysis differs significantly from subsequent analyses of the same inclusion, but most fall within deviation about the mean of measurements obtained under constant ablation of the fluid. In Figure 4B, most of the individual points lie within the deviation about the mean for ^{88}Sr, but for ^{85}Rb, four points differ significantly. Assuming that points with means outside the shaded regions are not acceptable, the results suggest that there is a 70-90% probability that the intensities measured from a small fluid inclusion will be accurate.

With respect to first breach intensities, most of the fluid inclusions listed in Table 2 exhibited a spike in their first breach intensities, with SE-15A and SE-15B showing deviations outside the mean (Figure 4). For the other four inclusions, the intensity spikes were within the uncertainties obtained by constant ablation. The data, though few in number, suggest that the first breach analysis will agree with the true analysis within error 66% of the time, for the conditions outlined in this study.

Geological implications

The most surprising result of this study is that Zn and Ag concentrations were below detection limits (< 10 ng ml^{-1}) in all fluid inclusions analysed. The results suggest that, by the time hydrothermal fluids precipitate gangue minerals, nearly all Zn and Ag have been removed. This agrees with observations that quartz occurs late in the paragenetic sequence at Santa Eulalia, i.e. after the bulk of Zn and Ag mineralisation. In contrast, Rb and Sr are at high levels in the last available fluids (Table 2). Rb and Sr concentrations vary between crystals, and between fluid inclusions in single crystals, suggesting that the quartz formed under conditions near the critical endpoint of H_2O, where element solubilities can fluctuate significantly (Norton 1984).

Summary

The calibration technique based on microcapillary tube solutions can be extended for use in the analysis of hydrothermal fluid inclusions. Care should be taken in interpreting results from single analyses in which the entire fluid inclusion volume is consumed, as significant deviations from the true element intensities can occur when the fluid inclusion is first breached. Future fluid inclusion studies will incorporate the addition of NaCl to fluid inclusion calibration solutions, to better approximate densities for natural hydrothermal fluids. The hydrothermal fluids trapped in late quartz at Santa Eulalia are depleted in Zn and Ag, with high levels of Rb and Sr. This suggests that most base metals are stripped from hydrothermal solutions during base metal sulfide mineralisation, leaving behind incompatible elements in the fluids.

Acknowledgments

This research was supported by collaborative NSF grants EAR-95-05982 to Ruiz and McCandless, and EAR-95-06023, EAR-94-05716 to A. M. Ghazi.

References

Anderson A.J. , Clark A.H. , Max P. , Palmer G.R. , MacArthur J.D. , Bodnar R.J. and Roedder E. (1987) *In situ* elemental analysis of fluid inclusion using PIXE and PIGMI. **Geological Association of Canada/Mineralogical Association of Canada Programs with Abstracts, 12,** 21.

Ayora C. and Fontarnau R. (1990) X-ray microanalysis of frozen fluid inclusions. **Chemical Geology, 89,** 135-148.

references

Boiron M.C. , Dubessy J. , Briand A. , Mauchien P. and Allé P. (1992)
Analysis of mono-atomic ions in individual fluid inclusions: A comparative study using LPES and SIMS PACROFI IV. University of California Conference Centre, Lake Arrowhead, California, USA, May 1992, 17.

Diamond L.W. , Marshall D.D. , Jackman J.A. and Skippen G.B. (1990)
Elemental analysis of fluid inclusions in minerals by secondary ion mass spectrometry (SIMS): Application to cation ratios of fluid inclusions in an Archaean meso-thermal gold-quartz vein. Geochimica et Cosmochimica Acta, 54, 545-552.

Frantz J.D. , Mao H.K. , Zhang Y.G. , Wu Y. , Thompson A.C. , Underwood R. , Gaiuque J.H. , Jones K.W. and Rivers M.L. (1988)
Analysis of fluid inclusions by X-ray fluorescence using synchrotron radiation. Chemical Geology, 69, 235-244.

Ghazi A.M. , McCandless T.E. , Vanko D.A. and Ruiz J. (1996)
New quantitative approach in trace elemental analysis of single fluid inclusion: Applications of laser ablation inductively coupled plasma-mass spectrometry (LA-ICP-MS). Journal of Analytical Atomic Spectrometry, 11, 667-674.

Horn I. E. and Tye C. E. (1989)
Analysis of fluid inclusions in minerals by VG laser ablation ICP-MS. PACROFI Programs with Abstracts, Virginia Polytechnic Institute and State University, USA, 32.

Irwin J.J. and Roedder E. (1995)
Diverse origins of fluid in magmatic inclusions at Bingham (Utah, USA), Butte (Montana, USA), St . Austell (Cornwall, UK), and Ascension Island (Mid-Atlantic, UK), indicated by laser microprobe analysis of Cl, K, I, Ba, Te, Ar, Kr, and Xe. Geochimica et Cosmochimica Acta, 59, 295-312.

Kelly W.C. and Burgio P.A. (1983)
Cryogenic scanning electron microscopy of fluid inclusions in ore and gangue minerals. Economic Geology 87, 1262-1267.

Mavrogenes J.A. , Bodnar R.J. , Anderson A.J. , Bajt S. , Sutton S.R. and Rivers M.L. (1995)
Assessment of the uncertainties and limitations of quantitative elemental analysis of fluid inclusions using synchrotron X-ray fluorescence (SXRF). Geochimica et Cosmochima Acta, 59, 3987- 3995.

Moissette A. , Shepherd T.J. and Chenery S. (1996)
Calibration strategies for the optimisation of laser ablation ICP-MS for the analysis of individual fluid inclusions. Journal of Analytical Atomic Spectroscopy, 11, 177-185.

Nambu M. , Sato T. , Hayakawa N. and Ohmori Y. (1977)
On the microanalysis of fluid inclusions with the ion microanalyser. Mining Geology (Japan), 27, 40.

Norton D.L. (1984)
Theory of hydrothermal systems. Annual Reviews of Earth and Planetary Sciences, 12, 155-177.

Ramsey M.H. , Coles B.J. , Rankin A.H. and Wilkinson J.J. (1992)
Single fluid inclusion analysis by laser ablation inductively coupled plasma-atomic emission spectrometry: Quantification and validation. Journal of Analytical Atomic Spectrometry, 7, 587-594.

Rankin A.H. , Ramsey M.H. , Coles B. , Van Langevelde F. and Thomas C.R. (1992)
The composition of hypersaline, iron-rich granitic fluids based on laser-ICP and synchrotron-XRF microprobe analysis of individual fluid inclusions in topaz, Mole granite, eastern Australia. Geochimica et Cosmochimica Acta, 56, 67-79.

Roedder E. (1984)
Fluid inclusions. Reviews in Mineralogy Volume 12, Mineralogical Society of America, Washington, DC, 644 pp.

Shepherd T.J. and Chenery S.R. (1995)
Laser ablation ICP-MS elemental analysis of individual fluid inclusions: an evaluation study. Geochimica et Cosmochimica Acta, 59, 3997-4007.

Vanko D.A. , Sutton S.R. , Rivers M.L. and Bodnar R.J. (1993)
Major-element ratios in synthetic fluid inclusions by synchrotron X-ray fluorescence microprobe. Chemical Geology, 107, 125-134.

Wilkinson J.J. , Rankin A.H. , Mulshaw S.C. , Nolan J. and Ramsey M.H. (1994)
Laser ablation ICP-AES for the determination of metals in fluid inclusions: An application to the study of magmatic ore fluid. Geochimica et Cosmochimica Acta, 58, 1133-1146.